

[PPh₄][V(HIDA)₂]-CH₂Cl₂ and [PPh₄][Δ-V((S,S)-HIDPA)₂]-H₂O were obtained by crystallization from CH₂Cl₂ and H₂O, respectively. The structures of these and related¹⁹ anions correspond closely to that of their V^{IV} counterpart in [NH₄][NMe₆][V(HIDA)₂].¹⁴ Figure 1 shows the geometry of [Δ-V((S,S)-HIDPA)₂]⁻; the stereochemistry at the metal is designated Δ by considering the relative positions of the two VON triangles as viewed perpendicular to the VO₄ plane. Overall, both complexes possess idealized C₂ symmetry. The vanadium-ligand distances for [V(HIDA)₂]ⁿ⁻ (n = 1, 2) and [Δ-V((S,S)-HIDPA)₂]⁻ (Table I) show that oxidation results in a significant contraction of one V-O(6) bond and a modest contraction of three V-O_{carboxylate} bonds, but no significant change in the V-O_{N₂hydroxyimino} distances. Thus, the SOMO of the V^{IV} systems is located in the VO₄ plane.

XAS have been recorded for *Amanita muscaria* and several of its chemical relatives.²⁰ The general lack of a pre-edge feature contrasts with observations for systems containing one (or more) V=O groups.²²⁻²⁴ The EXAFS of the synthetic systems is well interpreted by back-scattering from 6 O, 2 N, 8 C, and 4 O atoms at the crystallographic distances with inclusion of multiple scattering for the outer shell. The EXAFS for V^{IV} Amavadin is simulated successfully by back-scattering from 6 oxygens at 2.01 Å, 2 nitrogens at 2.04 Å, 8 carbons at 2.94 Å, and 4 oxygens at 4.0 Å with no indication of a short V=O contribution.

Cyclic voltammetry of Amavadin and its chemical analogues (refs 11 and 13, and this work) indicates that each of the V^{IV}/V^V pairs possesses a common geometry in solution. [V(HIDA)₂]⁻ manifests ¹H and ¹³C NMR spectra consistent with retention of the molecular geometry in solution; the ⁵¹V resonance is at -263 ppm vs VOCl₃. The ¹H and ¹³C NMR spectra of [Δ-V((S,S)-HIDPA)₂]⁻ are consistent with the structure (Figure 1) persisting in solution, and the ⁵¹V resonance is at -281 ppm. The ¹H NMR spectrum of oxidized Amavadin displays four doublets in the methyl region coupled to four quartets in the methine region; the relative integrals within these sets are approximately equal. Analogous sets of four resonances are seen in the ¹³C NMR spectrum and a single ⁵¹V resonance is observed at -280 ppm. The two doublets and two quartets seen in the ¹H NMR spectrum of [Δ-V((S,S)-HIDPA)₂]⁻, and the sets of two resonances seen in the ¹³C NMR spectrum, can be overlaid with half of the corresponding features of oxidized Amavadin. Therefore, oxidized Amavadin possesses two ligands with the same stereochemistry coordinated to the vanadium as in [V(HIDA)₂]ⁿ⁻ (n = 1, 2) and [V((S,S)-HIDPA)₂]⁻, but consists of an approximately equal mixture of the Δ and Λ forms of [V((S,S)-HIDPA)₂]⁻.

This conclusion is consistent with optical spectra. Oxidized and reduced Amavadin each manifest an electronic absorption spectrum which is essentially the same as the equivalent spectrum from

an HIDPA complex. However, the CD spectra of the oxidized and reduced forms of Amavadin have profoundly different sign distributions from those of the corresponding state of [Δ-V((S,S)-HIDPA)₂]ⁿ⁻ (n = 1, 2). Furthermore, a CD spectrum identical to that of reduced Amavadin can be obtained by reducing [Δ-V((S,S)-HIDPA)₂]⁻ with Na₂S₂O₄ and allowing the solution to stand for several hours. Reoxidation with [NH₄]₂[Ce(NO₃)₆] produces CD and ¹H and ¹³C NMR spectra identical to those of oxidized Amavadin. Thus, [Δ-V((S,S)-HIDPA)₂]²⁻ racemizes at the V^{IV} center.

These studies not only establish the chemical nature of Amavadin but also demonstrate that this species belongs to the group of transition metal centers in biology (e.g., blue copper, cytochromes, iron-sulfur) which retain their structure through a one-electron redox change.

Acknowledgment. We thank The Royal Society (D.C.), SERC and Unilever Research (L.J.C.), Carnegie Foundation (J.H.N.), and the University of Ege (N.E.) for funding and The Director of the SERC Daresbury Laboratory, Professor R. D. Gillard, and Dr. P. D. Newman for provision of facilities.

Kinetic, Spectroscopic, and Structural Evidence for Carbene-Carbyne Intermediates in Carbyne/CO Coupling

John D. Protasiewicz, Axel Masschelein, and Stephen J. Lippard*

Department of Chemistry
Massachusetts Institute of Technology
Cambridge, Massachusetts 02139

Received September 11, 1992

Understanding the intimate mechanism of carbon-carbon bond formation between two ligands in an organometallic complex is of fundamental interest. Coupling of carbyne and CO or CNR ligands has become a general class of such reactions.¹⁻⁵ Both η²-ketenyl and carbene-carbyne intermediates have been shown or postulated to be involved in the key C-C bond forming step.⁶⁻⁹ Recently we demonstrated that the reductive coupling of CO ligands in [M(CO)₂(dmpe)₂Cl] (M = V, Nb, or Ta) to form [M(R₃SiOC≡COSiR₃)(dmpe)₂X] occurs via sequential formation of Na[M(CO)₂(dmpe)₂] and [M(≡COSiR₃)(CO)(dmpe)₂] complexes.⁹⁻¹¹ In order to elucidate further details of the coupling step, we have undertaken the first kinetic study of carbyne/CO coupling. Here we report that the rate-determining step of the reaction of [Ta(≡COSiPr₃)(CO)(dmpe)₂] (1) with Me₃SiCl to form [Ta(Pr₃SiOC≡COSiMe₃)(dmpe)₂Cl] (2)⁹ involves electrophilic attack by the silyl reagent upon the terminal CO ligand

(18) [PPh₄][Δ-V((S,S)-HIDPA)₂]-H₂O crystallizes in the orthorhombic space group P2₁2₁2₁; a = 1530 (1), b = 2818 (2), c = 854.6 (5) pm, V = 3685 (4) × 10⁶ pm³, Z = 4; F(000) = 1576, ρ_{calcd} = 1.363 g cm⁻³; μ = 3.60 cm⁻¹; Mo Kα radiation, 2θ_{max} = 39.9°; 2107 reflections measured, 1837 observed (I > 3σI); number of parameters 460; R = 0.068, R_w = 0.093.

(19) The crystal structures of [PPh₄][V((R,S)-HIDPA)₂]-CH₂Cl₂ and [PPh₄][V((R,S)-HIDPA)((S,S)-HIDPA)]-CH₂Cl₂ have also been determined. These anions possess a set of bond lengths similar to those detailed for the vanadium(V) complexes in Table I.

(20) Vanadium K-edge X-ray absorption spectra (XAS) were recorded on stations 7.1 and 8.1 of the Daresbury Synchrotron Radiation Source for *Amanita muscaria* extract (ex. Sigma), an aqueous solution of Amavadin in its V^{IV} state, a CH₂Cl₂ solution of Amavadin oxidized by treatment with [NH₄]₂[Ce(NO₃)₆], and solid samples of [NH₄][NMe₆][V(HIDA)₂], H₂[V((R,S)-HIDPA)₂], [PPh₄][V(HIDA)₂]-CH₂Cl₂, and [PPh₄][V((R,S)-HIDPA)₂]-CH₂Cl₂. The energy of the vanadium K-edge²¹ was found to be 5480.8 and 5482.4 ± 0.3 eV for the vanadium(IV) and -(V) centers, respectively, consistent with the variation expected²²⁻²⁴ between these oxidation states, although the values are slightly higher than the corresponding edge positions of oxovanadium(IV) and -(V) compounds.

(21) The position of the vanadium K-edge was taken as the first point of inflection on the edges and referenced to that of vanadium foil at 5466 eV.

(22) Wong, J.; Lytle, F. W.; Messmer, R. P.; Maylotte, D. H. *Phys. Rev.* **1984**, *B30*, 5596.

(23) Hallmeier, K. H.; Szargan, R.; Werner, G.; Meier, R.; Sheromov, M. A. *Spectrochim. Acta* **1986**, *42A*, 841.

(24) Arber, J. M.; de Boer, E.; Garner, C. D.; Hasnain, S. S.; Wever, R. *Biochemistry* **1989**, *28*, 7968.

(1) Mayr, A. *Comments Inorg. Chem.* **1990**, *10*, 227.

(2) Mayr, A.; Hoffmeister, H. *Adv. Organomet. Chem.* **1991**, *32*, 227.

(3) Mayr, A.; Bastos, C. M. *Prog. Inorg. Chem.* **1992**, *40*, 1.

(4) Vrtis, R. N.; Lippard, S. J. *Isr. J. Chem.* **1990**, *30*, 331.

(5) Carnahan, E. M.; Protasiewicz, J. D.; Lippard, S. J. *Acc. Chem. Res.*, in press.

(6) We refer to the latter species as carbene-carbynes, rather than bis carbynes, since d-block transition metal complexes do not have enough orbitals to form two independent metal-carbon triple bonds. To emphasize the symmetrical nature of the related isocyanide-derived species, however, these complexes have also been described as bis(carbynes). There are, of course, several resonance forms that can be drawn to describe the bonding in such complexes. See also: (a) Brower, D. C.; Templeton, J. L.; Mingos, D. M. P. *J. Am. Chem. Soc.* **1987**, *109*, 5203. (b) Wilker, C. N.; Hoffmann, R.; Eisenstein, O. *Nouv. J. Chem.* **1983**, *7*, 535.

(7) Filippou, A. C.; Völkl, C.; Grünleitner, W.; Kiprof, P. *J. Organomet. Chem.* **1992**, *434*, 201.

(8) Filippou, A. C.; Grünleitner, W.; Völkl, C.; Kiprof, P. *Angew. Chem., Int. Ed. Engl.* **1991**, *30*, 1167.

(9) Vrtis, R. N.; Liu, S.; Rao, C. P.; Bott, S. G.; Lippard, S. J. *Organometallics* **1991**, *10*, 275.

(10) Bianconi, P. A.; Vrtis, R. N.; Rao, C. P.; Williams, I. D.; Engeler, M. P.; Lippard, S. J. *Organometallics* **1987**, *6*, 1968.

(11) Protasiewicz, J. D.; Lippard, S. J. *J. Am. Chem. Soc.* **1991**, *113*, 6564.

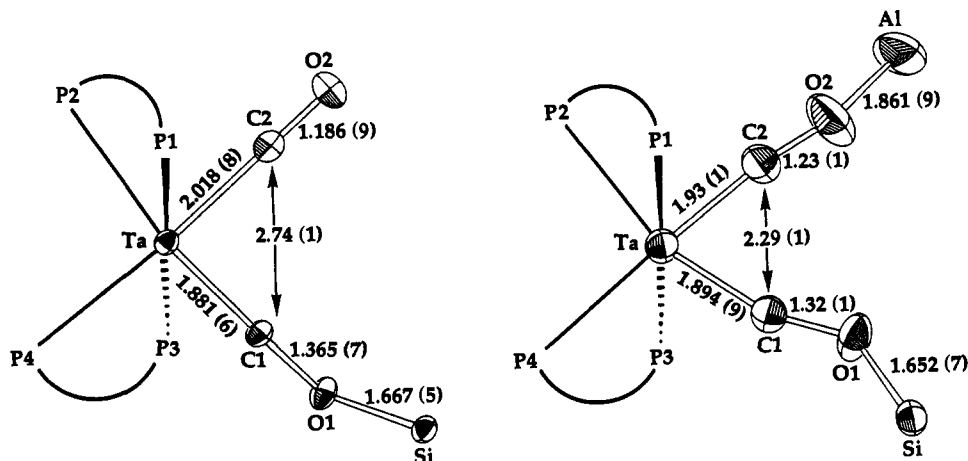
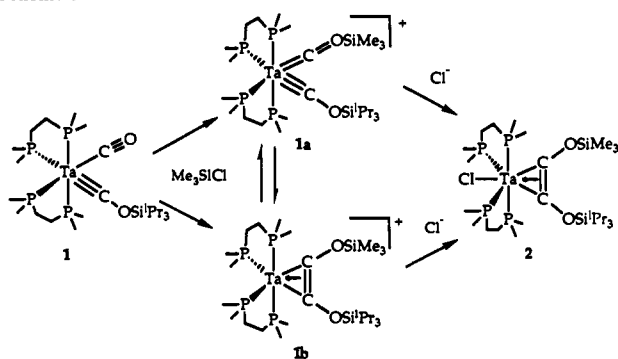


Figure 1. Structural diagrams of **3** (left) and **4** (right), showing 30% probability thermal ellipsoids and distances in angstroms for selected atoms. Important bond angles (deg) for **3**: C1-Ta-C2, 89.1 (1); Ta-C1-O1, 168.3 (5); C1-O1-Si, 127.1 (4); Ta-C2-O2, 179.5 (6); P2-Ta-C2, 81.5 (2); P2-Ta-P4, 95.97 (7); P4-Ta-C1, 96.2 (2). For **4**: C1-Ta-C2, 73.4 (4); Ta-C1-O1, 162.4 (7); C1-O1-Si, 135.9 (6); Ta-C2-O2, 172.8 (9); C2-O2-Al, 144.1 (8); P2-Ta-C2, 88.2 (3); P2-Ta-P4, 94.2 (1); P4-Ta-C1, 105.3 (3).

Scheme I



of **1**. This conclusion is supported by the first-order dependence of the reaction upon each reagent and the large rate accelerations observed upon addition of tetraalkylammonium salts to the reaction medium. The silylated intermediate has been modeled by addition of AlEt_3 to $[\text{Ta}(\equiv\text{COSi}^i\text{BuPh}_2)(\text{CO})(\text{dmpe})_2]$ (**3**) to form $[\text{Ta}(\equiv\text{COSi}^i\text{BuPh}_2)(\text{COAlEt}_3)(\text{dmpe})_2]$ (**4**), the structure of which is both surprising and revealing.

Reaction of deep red **1** with excess Me_3SiCl in THF to afford green $[\text{Ta}(\text{R}_3\text{SiOC}\equiv\text{COSiR}_3)(\text{dmpe})_2\text{Cl}]^9$ was followed in a stopped-flow apparatus by monitoring the decrease in optical density at 480 nm. Addition of either (*n*-pentyl) $_4\text{NCl}$ or (*n*-butyl) $_4\text{NBPh}_4$ substantially increased the observed pseudo-first-order rate constant(s), suggesting that either a charged transition state or intermediate is involved.¹² At a constant salt concentration, the reaction was not accelerated by chloride ion, eliminating a pathway involving halide-induced η^2 -ketenyl formation.¹³ Since the reaction is first order in both **1** and Me_3SiCl under these conditions, the rate-determining step of the reaction involves silylation of the terminal CO ligand (Scheme I).¹⁴ The second-order rate constant was determined to be $1.71 \pm 0.04 \text{ M}^{-1} \text{ s}^{-1}$ at $22 \pm 1 \text{ }^\circ\text{C}$ ($[(n\text{-butyl})_4\text{NBPh}_4]$, 23.9 mM).

(12) Reactions of two neutral species to form a charged transition state are expected to be accelerated by increasing the ionic strength of the medium, especially when carried out in a solvent of low dielectric constant, such as THF. See: (a) Connors, K. A. *Chemical Kinetics. The Study of Reaction Rates in Solution*; VCH Publishers, Inc.: New York, 1990. (b) Zuman, P.; Patel, R. C. *Techniques in Organic Reaction Kinetics*; John Wiley & Sons: New York, 1984.

(13) Although chloride ion does not promote η^2 -ketenyl formation, it does catalyze scrambling of the silyl groups. Thus, reaction of **1** with Me_3SiCl in the presence of chloride yields $[\text{Ta}(\text{Me}_3\text{SiOC}\equiv\text{COSiMe}_3)(\text{dmpe})_2\text{Cl}]$ rather than **2**. Full details will be presented elsewhere.

(14) Another formal possibility is that **1** is in rapid equilibrium with a small amount of a 16-electron η^2 -ketenyl complex which is trapped in the rate-determining step by Me_3SiCl . If such a species were to exist, however, it should also react with electrophiles such as AlEt_3 (see text below).

These kinetic results do not indicate whether carbon-carbon bond formation occurs in the rate-determining step (Scheme I, upper vs lower pathways). The effect of Lewis acid binding to **1** was therefore explored to afford additional insight. Addition of AlEt_3 to a toluene solution of **1** resulted in an immediate color change from deep red to a light red/orange and produced a dramatic shift in ν_{CO} from 1790 to 1605 cm^{-1} . Although crystals of this complex suitable for a X-ray structural analysis could not be obtained, the structures of the analogous pair of complexes $[\text{Ta}(\equiv\text{COSi}^i\text{BuPh}_2)(\text{CO})(\text{dmpe})_2]$ (**3**) and $[\text{Ta}(\equiv\text{CO-Si}^i\text{BuPh}_2)(\text{COAlEt}_3)(\text{dmpe})_2]$ (**4**) were successfully determined. Figure 1 displays a view in the coupling plane³ of both molecules.¹⁵ The structure of **3** is similar to that previously reported for **1**.⁹ Complex **4** reveals several interesting geometric features as compared to **3**. Addition of the aluminum reagent to the terminal CO ligand decreases the metal-carbon bond length by 0.09 (1) Å and increases the C-O distance by 0.04 (1) Å. These bond length attenuations are also reflected by the changes in the IR spectra on going from **3** (ν_{CO} 1793 cm^{-1}) to **4** (ν_{CO} 1579 cm^{-1}).¹⁶ Complex **4** is therefore best described as a Fischer type carbene-carbyne complex and appears to be the first structurally characterized example of such a complex.^{17,18} A surprising feature of **4** is that the angle between the two unsaturated fragments has decreased from 89.1 (3) $^\circ$ in **3** to 73.4 (4) $^\circ$, bringing the corresponding distance between the two metal-bound carbon atoms to 2.29 (1) Å. This value is reminiscent of the close non-bonded contacts observed in seven-coordinate complexes of the type $[\text{M}(\text{CO})_2(\text{dmpe})_2\text{X}]$ (M = Nb or Ta).¹⁹

Addition of chloride ion to toluene solutions of the above carbene-carbyne species did not result in C-C coupling; instead, the starting carbene-CO complexes were regenerated. This result suggests that halide addition to the transition metal center, rather than to the aluminum or silicon atoms, may require a positively charged complex, such as **1a**. The ability to isolate the alumin-

(15) Full structural details and ORTEP diagrams of **3** and **4** are available as supplementary material.

(16) For a review of Lewis acid adducts of CO ligands, see: Horwitz, C. P.; Shriver, D. F. *Adv. Organomet. Chem.* **1984**, *23*, 219.

(17) Schrock type carbynes having alkylidene ligands are well known. See: (a) Fischer, H.; Hofmann, P.; Kreissl, F. R.; Schrock, R. R.; Schubert, U.; Weiss, K. *Carbyne Complexes*; VCH Publishers: New York, 1988. (b) Nugent, W. A.; Mayer, J. M. *Metal-Ligand Multiple Bonds: The Chemistry of Transition Metal Complexes Containing Oxo, Nitrido, Imido, Alkylidene, or Alkylidene Ligands*; Wiley: New York, 1988.

(18) Two related structures have been described. See: (a) Conway, A. J.; Gainsford, G. J.; Schrieke, R. R.; Smith, J. D. *J. Chem. Soc., Dalton Trans.* **1975**, 2499. (b) Merola, J. S.; Campo, K. S.; Gentile, R. A.; Modrick, M. A.; Zentz, S. *Organometallics* **1984**, *3*, 334.

(19) Protasiewicz, J. D.; Bianconi, P. A.; Williams, I. D.; Liu, S.; Rao, C. P.; Lippard, S. J. *Inorg. Chem.* **1992**, *31*, 4134.

oxy-siloxy carbene-carbynes (cf. refs 20 and 21) parallels the reported stability of bis(dialkylamino)carbynes.^{6,8,22} We have thus far been unable to obtain the isoelectronic bis(siloxy)carbynes.^{6,23} Coupling of unsubstituted "bis-carbyne" fragments has been reported to occur spontaneously.^{24,25}

Some interesting questions remain to be answered for the present system. Addition of the aluminum reagent to **3** has brought the carbon atoms of the carbene-carbyne ligands of **4** closer together. Would a stronger electrophile (e.g., R_3Si^+) result in the distance closing to that required for acetylene formation (Scheme 1, **1** to **1b**)? Does the extent of the interaction of the electrophile determine the position of the equilibrium illustrated in Scheme 1 (**1a** \rightleftharpoons **1b**), or does C-C bond formation require addition of a nucleophile to the metal to drive the carbene-carbyne ligands together in a seven-coordinate complex to accomplish coupling (**1a** to **2**)?⁵ Experiments are in progress to address these issues.

Acknowledgment. This work was supported by a grant from the National Science Foundation. We are grateful to the George R. Harrison Spectroscopy Laboratory for allowing us access to their facility supported by NSF (CHE-8914953) and NIH (P41RR02594). A.M. thanks NATO and C.I.E.S. for fellowships and J.D.P. support from Training Grant CA 09112 from the National Cancer Institute.

Supplementary Material Available: Tables of rate data and reaction order plots, listings of full characterization and experimental details for **3** and **4**, complete ORTEP diagrams of **3** and **4**, and tables of positional and thermal parameters (24 pages). Ordering information is given on any current masthead page.

(20) Churchill, M. R.; Wasserman, H. J.; Holmes, S. J.; Schrock, R. R. *Organometallics* **1982**, *1*, 766.

(21) Holmes, S. J.; Schrock, R. R.; Churchill, M. R.; Wasserman, H. J. *Organometallics* **1984**, *3*, 476.

(22) Chatt, J.; Pombeiro, A. J. L.; Richards, R. L. *J. Chem. Soc., Dalton Trans.* **1980**, 492.

(23) The formation of $[V(Me_2SiOC\equiv COSiMe_2)(dmpe)_2]OTf$ from the reaction of $Na[V(CO)_2(dmpe)_2]$ and Me_2SiOTf may be the result of the instability of such a bis-siloxy(carbyne)⁶ undergoing spontaneous coupling. See ref 11.

(24) McDermott, G. A.; Mayr, A. *J. Am. Chem. Soc.* **1987**, *109*, 580.

(25) Mayr, A.; Bastos, C. M.; Daubenspeck, N.; McDermott, G. A. *Chem. Ber.* **1992**, *125*, 1583.

Nitric Oxide-Triggered Heme-Mediated Hydrolysis: A Possible Model for Biological Reactions of NO

Teddy G. Traylor,* Arthur F. Duprat, and Vijay S. Sharma

Departments of Medicine and Chemistry
University of California at San Diego
9500 Gilman Drive, La Jolla, California 92093-0506

Received September 18, 1992

The recent discoveries of wide-ranging physiological effects of nitric oxide,¹⁻¹² in most cases associated with the enzyme guanylate cyclase,¹³ have stimulated increased interest in the chemistry and

(1) Moncada, S.; Palmer, R. M. J.; Higgs, E. A. *Pharm. Rev.* **1991**, *43*, 109-141.

(2) Crossin, K. L. *Trends Biochem. Sci.* **1991**, 81-82.

(3) McCall, T.; Vallance, P. *Trends Pharmacol. Sci.* **1992**, *13*, 1-6.

(4) Garthwaite, J. *Trends Neurosci.* **1991**, *14*, 60-67.

(5) Nowak, R. *J. NIH Res.* **1992**, *4*, 49-55.

(6) Rajfer, J.; Aronson, W. J.; Bush, A.; Dorey, F. J.; Ignarro, L. J. *New Eng. J. Med.* **1992**, *326*, 90-94.

(7) Barinaga, M. *Science* **1991**, *254*, 1296-1297.

(8) Palmer, R. M. J.; Ferrige, A. G.; Moncada, S. *Nature* **1987**, *327*, 524-526.

(9) Luscher, T. F.; Richard, V.; Tanner, F. C. *Trends Cardiovasc. Med.* **1991**, *1*, 179-185.

(10) Ignarro, L. J. *Semin. Hematol.* **1989**, *26*, 63-76.

(11) Ignarro, L. J. *Circ. Res.* **1989**, *65*, 1-21.

(12) Ignarro, L. J. *J. NIH Res.* **1992**, *4*, 59-62.

(13) Gerzer, R.; Böhme, E.; Hofmann, F.; Schultz, G. *FEBS Lett.* **1981**, *132*, 71-74.

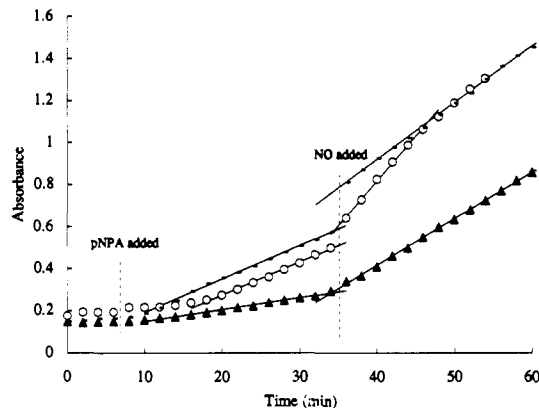
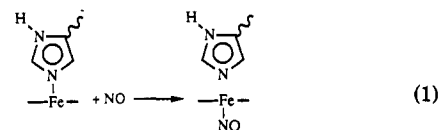
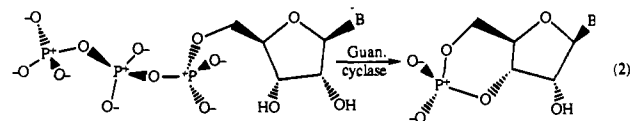


Figure 1. Absorbance of *p*-nitrophenolate (405 nm) in the aqueous phase (3 mL) stirred with dichloromethane solutions: (○) MCPH-CO (5 μ mol) in dichloromethane (0.3 mL); (▲) 1-Melm-Hm-CO heme (5 μ mol) in 0.3 mL of dichloromethane; (○) 1-Melm-Hm-CO (10 μ mol) in dichloromethane (0.3 mL). The substrate (pNPA, 25 μ mol in 50 μ L of dichloromethane) and NO gas (2 mL) were added at the points indicated.

biology of nitric oxide.¹⁴⁻¹⁷ The UV-vis spectrum of guanylate cyclase, which contains a rather loosely bound five-coordinated protoheme,¹³ changes from one which resembles ferrous myoglobin to a species with a Soret band at 399 nm upon addition of nitric oxide.^{13,18} This change is attributed to the loss of the proximal



base (eq 1). The corresponding reaction of myoglobin gives a six-coordinate complex ($\lambda_{\text{max}} = 419 \text{ nm}$).¹⁹ The spectroscopic change in guanylate cyclase is accompanied by an activation of this enzyme, resulting in the conversion of GTP to cyclic GMP.³⁻¹³



The process in eq 1 suggests two possible mechanisms for catalysis of the reaction. Either the released imidazole acts as a general or nucleophilic catalyst²⁰ or the breaking of the iron-imidazole bond results in a change to another enzyme conformation which favors GTP binding and possibly aids in the catalytic steps. The first mechanism is particularly attractive if the catalytic site is near the heme, as has been suggested by Ignarro et al.²¹ Examples of heme-induced conformational change are numerous; a possible model system for this type of mechanism was recently suggested²² in which peptide helices were stabilized by binding a metal to two properly juxtaposed imidazoles.

We present here a model for the first mechanism and demonstrate NO-triggered catalysis of a hydrolysis reaction. We have

(14) Traylor, T. G.; Sharma, V. S. *Biochemistry* **1992**, *31*, 2847-2849.

(15) Murphy, M. E.; Sies, H. *Proc. Natl. Acad. Sci. U.S.A.* **1991**, *88*, 10860-10864.

(16) Sharma, V. S.; Traylor, T. G.; Gardiner, R.; Mizukami, H. *Biochemistry* **1987**, *26*, 3837-3843.

(17) Ignarro, L. J.; Adams, J. B.; Horwitz, P. M.; Wood, K. S. *J. Biol. Chem.* **1986**, *261*, 4997-5002.

(18) Rose, E. J.; Hoffman, B. M. *J. Am. Chem. Soc.* **1983**, *105*, 2866-2873.

(19) Wittenberg, J. B.; Noble, R. W.; Wittenberg, B. A.; Antonini, E.; Brunori, M.; Wyman, J. *J. Biol. Chem.* **1967**, *242*, 626-634.

(20) Anslyn, E.; Breslow, R. *J. Am. Chem. Soc.* **1989**, *111*, 4473-4482.

(21) Ignarro, L. J.; Kadowitz, P. J.; Baricos, W. H. *Arch. Biochem. Biophys.* **1981**, *208*, 75-86.

(22) Ghadiri, M. R.; Fernholz, A. K. *J. Am. Chem. Soc.* **1990**, *112*, 9633-9635.